Redox and Src family kinase signaling control leukocyte wound attraction and neutrophil reverse migration

Sebastien Tauzin,[1] Taylor W. Starnes,[2] Francisco Barros Becker,[1,3] Pui-ying Lam,[1,3] and Anna Huttenlocher[1]

[1]Departments of Pediatrics and Medical Microbiology and Immunology, [2]Microbiology Doctoral Training Program and Medical Scientist Training Program, [3]Program in Cellular and Molecular Biology, University of Wisconsin-Madison, Madison, WI 53706

Tissue damage induces early recruitment of neutrophils through redox-regulated Src family kinase (SFK) signaling in neutrophils. Redox-SFK signaling in epithelium is also necessary for wound resolution and tissue regeneration. How neutrophil-mediated inflammation resolves remains unclear. In this paper, we studied the interactions between macrophages and neutrophils in response to tissue damage in zebrafish and found that macrophages contact neutrophils and induce resolution via neutrophil reverse migration. We found that redox-SFK signaling through p22phox and Yes-related kinase is necessary for macrophage wound attraction and the subsequent reverse migration of neutrophils. Importantly, macrophage-specific reconstitution of p22phox revealed that macrophage redox signaling is necessary for neutrophil reverse migration. Thus, redox-SFK signaling in adjacent tissues is essential for coordinated leukocyte wound attraction and repulsion through pathways that involve contact-mediated guidance.

Introduction

Tissue damage and repair involves the complex interactions between different populations of cells and their coordinated cell movement (Nathan, 2006; Silva, 2010; Sindrilaru and Scharffetter-Kochanek, 2013; Abtin et al., 2014). The mechanisms through which these interactions are orchestrated to mediate resolution of inflammation, a key step in tissue repair, remain largely unknown (Nathan and Ding, 2010). The resolution of neutrophil-mediated inflammation was classically thought to occur through controlled apoptosis (Ortega-Gómez et al., 2013). However, recent work has established that migration of neutrophils out of inflamed tissues, termed neutrophil reverse migration, is a key mechanism of local resolution (Mathias et al., 2006; Woodfin et al., 2011; Starnes and Huttenlocher, 2012; Robertson et al., 2014). Macrophages are known to regulate the resolution of neutrophil-mediated inflammation through phagocytosis of apoptotic neutrophils (Bratton and Henson, 2011). However, the role of macrophage–neutrophil interactions in reverse migration-mediated resolution is unknown. We took advantage of transparent zebrafish larvae to manipulate interactions between neutrophils and macrophages and identified a neutrophil-repelling role for macrophages during the resolution of neutrophil-mediated inflammation.

Results and discussion

To investigate how neutrophils and macrophages interact after tail wounding, a time course was performed in double transgenic larvae, Tg(*mpx:DsRed*) × Tg(*mpeg1:Dendra2*), which labels both neutrophils and macrophages, respectively (Fig. 1, A–C). In accordance with previous studies (Holmes et al., 2012; Li et al., 2012), we found that neutrophils and macrophages are recruited with different kinetics to tissue damage (Fig. 1 B; Ellett et al., 2011). Neutrophils are often the first cells to arrive at a wound, and macrophages subsequently accumulate along the wound margin. Surprisingly, we found an inverse correlation between neutrophil and macrophage numbers at the wound (Fig. 1 C). Real-time imaging using double labeling showed that after macrophages contact neutrophils at the wound edge, as

Correspondence to Anna Huttenlocher: Huttenlocher@wisc.edu

Abbreviations used in this paper: ANOVA, analysis of variance; CGD, chronic granulomatous disease; dpf, day postfertilization; DPI, diphenyliodonium; Duox, dual oxidase; hptt, hour post–tail transection; hpw, hour postwounding; MO, morpholino; ROS, reactive oxygen species; SFK, Src family kinase; Yrk, Yes-related kinase.

The Rockefeller University Press $30.00
J. Cell Biol. Vol. 207 No. 5 589–598
www.jcb.org/cgi/doi/10.1083/jcb.201408090

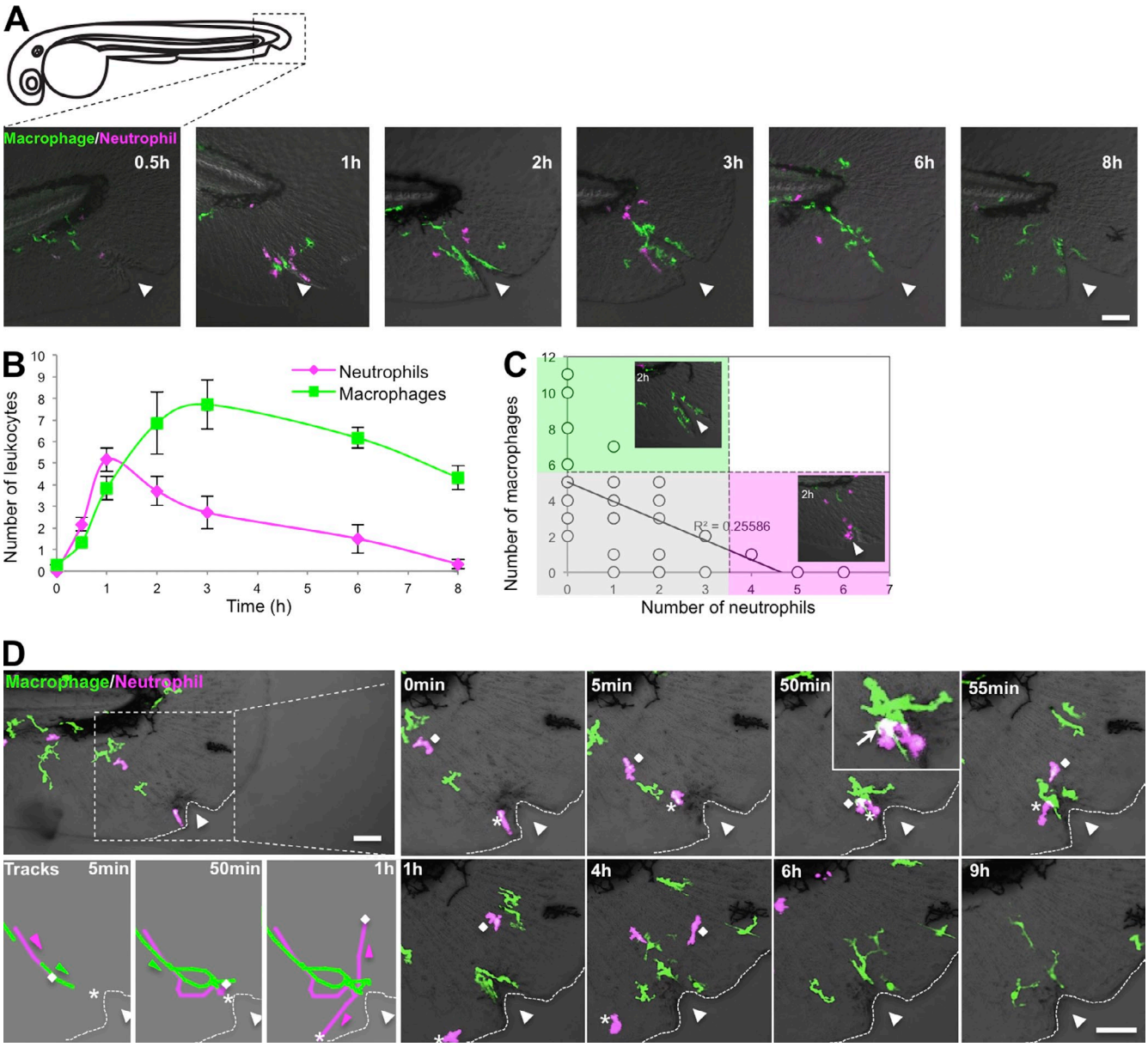

Figure 1. **Kinetics of neutrophil–macrophage interactions at wounds.** (A) Representative images of 3-dpf double transgenic larvae Tg(*mpx:DsRed*) × Tg(*mpeg1:Dendra2*) showing neutrophil and macrophage recruitment and resolution at the indicated times after needle wounding. (B) Quantification of the number of neutrophils and macrophages at wounds of larvae depicted in A. n = 43 larvae. Error bars indicate SEM. (C) Number of macrophages as a function of number of neutrophils at 1 and 2 hpw depicted in A. n = 43 larvae. Gray, macrophages and neutrophils are equally present at wound; green, macrophages predominate; pink, neutrophils predominate. (D) Real-time imaging of the leukocyte response to needle wounding using 3-dpf double transgenic Tg(*mpx:DsRed*) × Tg(*mpeg1:Dendra2*) larvae. Dotted lines delimit fins. Diamonds indicate neutrophil #1, and asterisks indicate neutrophil #2. Triangles indicate needle wound location. Bars, 50 µm.

indicated by regions of overlay, neutrophils migrate away from the macrophages, whereas macrophages persist at the wound edge (Fig. 1 D and Videos 1 and 2).

Cell tracking revealed that the kinetics of neutrophil behavior was different depending on the presence or absence of macrophages at the wound (Fig. 2 A and Video 3), with neutrophil mean duration at the wound reduced by ∼60 min when macrophages are present (Fig. 2 B). If neutrophils arrive at the wound first (in 16 out of 54 videos), they migrate randomly around the wound with periodic stopping and low relative velocity and directionality near the wound (Fig. 2 C). In contrast, if macrophages are present, neutrophils exhibit more directed migration at the wound, with increased velocity (in 23 out of 54 videos; Fig. 2 D), resulting in shorter durations at the wound. When neutrophils arrive first at the wound (condition a), every neutrophil (n = 20 neutrophils tracked from 16 different videos) was contacted by a macrophage before reverse migrating. When neutrophils come after macrophages (condition b), 61.7% (37/60 neutrophils tracked from 13 different videos) of the neutrophils contacted macrophages at the wound before reverse migrating. The remaining 38.3% (23/60 neutrophils tracked from 16 different videos) reverse migrated before any macrophage

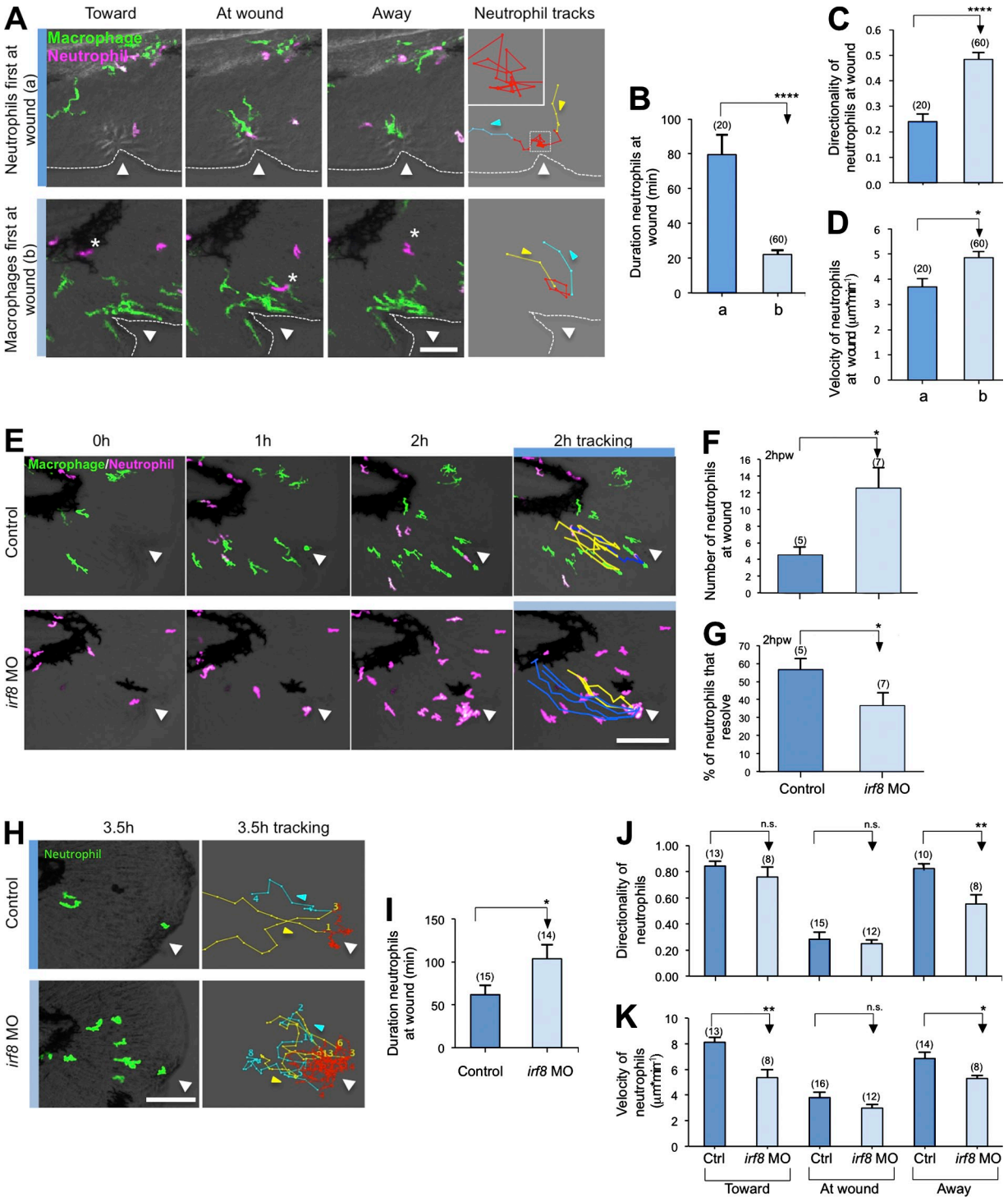

Figure 2. **Macrophages regulate neutrophil resolution at wounds.** (A) Real-time imaging of neutrophil behavior near wounds when neutrophils arrive first at the wound (a) or after macrophages (b) in 3-dpf Tg(*mpx:DsRed*) × Tg(*mpeg1:Dendra2*). Yellow lines indicate neutrophil tracks toward wounds, red line are tracks at wounds, and blue lines are tracks away from wounds. Dotted lines indicate the fin margin. The inset represents an enlargement of the dashed square. The asterisks identify the location of the same neutrophil at different time points. (B) Quantification of the duration that neutrophils stay at the wound in condition a and b. (C and D) Quantification of the directionality (C) and velocity (D) of neutrophils near the wound (red track) in condition a and b. In B–D, (*n*) = number of neutrophil tracks at the wound (red track) analyses for each condition. (E) Real-time imaging over 2 hpw in control or *irf8* morphant (*irf8* MO) Tg(*mpx:DsRed*) × Tg(*mpeg1:Dendra2*) larvae. Blue lines correspond to neutrophils that stay at wounds, and yellow lines correspond to neutrophils that resolve. (F) Number of neutrophils at wound 2 hpw in control and *irf8* MO larvae. (G) Percentage of neutrophils that resolved from the wounded zone during the 2 hpw in control and *irf8* MO larvae. In F and G, (*n*) = number of larvae. (H) Real-time imaging and neutrophil tracking in control or *irf8* MO Tg(*mpx:Dendra*) larvae from 0–3.5 hpw. Yellow lines indicate neutrophils migrating toward the wound, red line shows migration at the wound, and blue lines shows migration away from the wound. (I) Quantification of duration that neutrophils stay at the wound in control and *irf8* MO larvae. (J and K) Quantification of the directionality (J) and velocity (K) of neutrophils toward the wound, at the wound, and away from the wound in control and *irf8* MO larvae. In I–K, (*n*) = number of neutrophil tracks analyzed for each condition. Ctrl, control. Horizontal lines indicate means. Error bars indicate SEM. *, $P < 0.05$; **, $P < 0.01$; ****, $P < 0.0001$, two-tailed unpaired *t* test. Triangles indicate needle wound location. Bars: (A) 50 µm; (E and H) 100 µm.

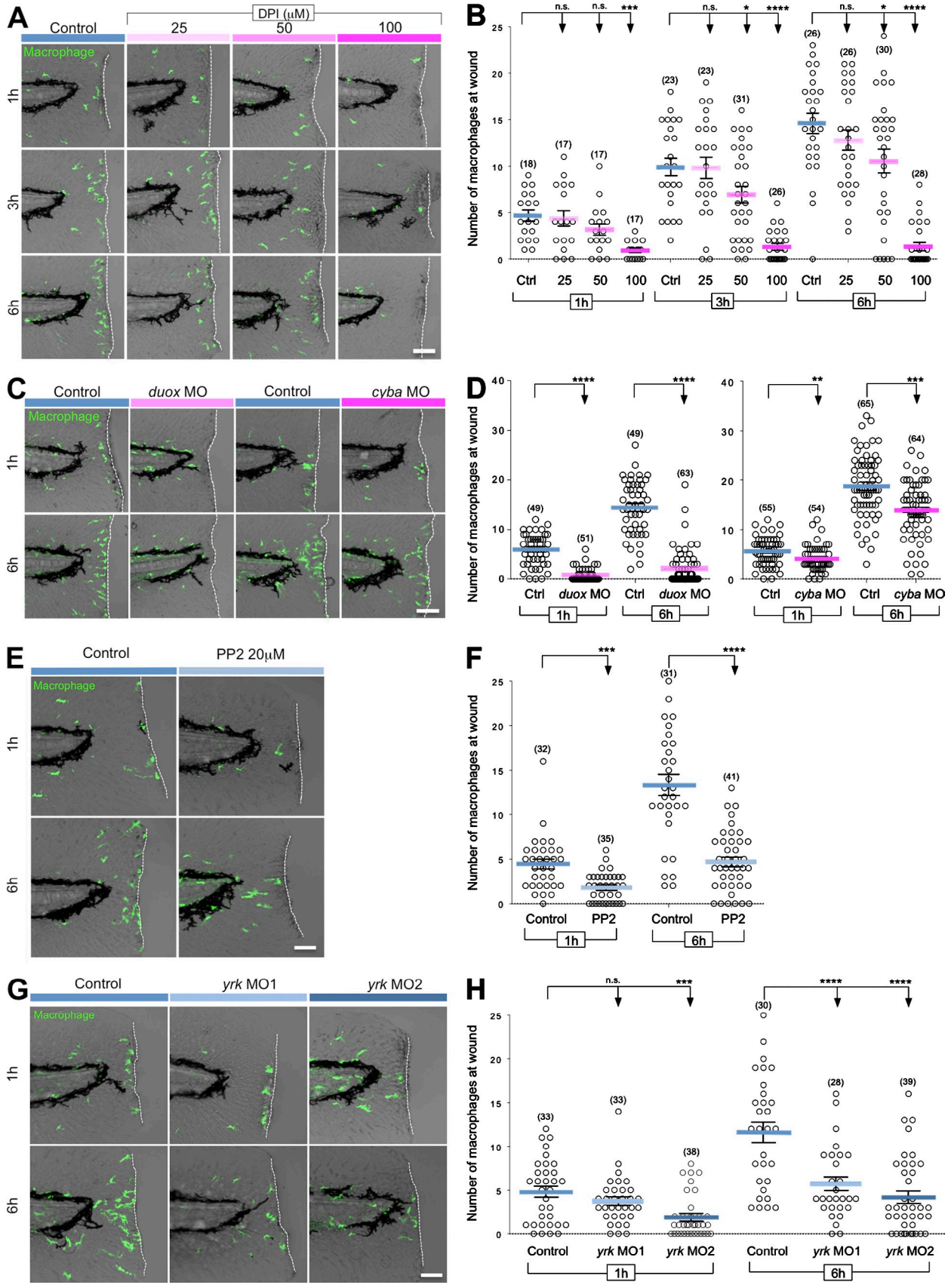

Figure 3. **ROS and SFKs mediate macrophage wound attraction.** (A) Representative images of 3-dpf Tg(*mpeg1:Dendra2*) larvae treated with increasing concentrations of the NADPH oxidase inhibitor DPI for 1, 3, and 6 hptt. (B) Quantification of macrophage recruitment to wounded fins after DPI treatment at the indicated times. (C) Representative images of control, *duox* morphant (*duox* MO), or *cyba* morphant (*cyba* MO) 3-dpf Tg(*mpeg1:Dendra2*)

contact. These findings suggest that, depending on context, not all macrophages play a repelling role. Macrophages occasionally were "distracted" from the wound and appeared to "chase" neutrophils (Fig. S1 A and Videos 4 and 5). In this case, neutrophils tried to "avoid" macrophage interactions and migrate away from the wound or approach the wound by a different route to avoid macrophage contact (Fig. S1 B and Video 6). In 9 out of 54 videos, macrophages chase and trap live neutrophils (Videos 7 and 8) and rarely phagocytose neutrophils as an alternative fate (2 out of 54 videos; Fig. S1 C and Video 7). This chase and run behavior is reminiscent of the recently reported interactions between neural crest and placode cells (Theveneau et al., 2013). The observation that wound-associated macrophages interact with neutrophils before neutrophil reverse migration suggests a role for macrophage-mediated repulsion in this process. These findings suggest that macrophages may influence neutrophil behavior at the wound in a type of contact inhibition (Fig. S1 D; Abercrombie, 1967), as has been reported during developmental cell movements and embryonic dispersal of *Drosophila melanogaster* hemocytes (Stramer et al., 2010).

To determine whether macrophages promote the resolution of neutrophil-mediated inflammation, we used a previously reported *irf8* morpholino (MO) to deplete larvae of macrophages (Li et al., 2011). Although *irf8* MO results in a dramatic increase in the total number of neutrophils, macrophage depletion also induced a relative increase of neutrophil number at wounds compared with control at later time points after wounding, indicating a defect in neutrophil resolution (Fig. S2, A–C). To determine whether the defect in resolution was caused by impaired neutrophil reverse migration, we tracked neutrophil fate in *irf8* morphants. At 2 h postwounding (hpw), 57% of neutrophils had undergone reverse migration in controls compared with only 35% in macrophage-deficient larvae (Fig. 2, E–G; and Video 9). The finding that neutrophils will still exhibit reverse migration in the absence of macrophages indicates that other factors are also involved in neutrophil reverse migration (Holmes et al., 2012; Starnes and Huttenlocher, 2012). Further tracking revealed that the duration that neutrophils remained at the wound was increased in *irf8* morphants and that the velocity and directionality of neutrophils moving away from the wound was reduced (Fig. 2, H–K; and Video 10). These results suggest that macrophages play an important role in guiding neutrophils, as further suggested by a recent study showing that perivascular macrophages mediate the recruitment of neutrophils to infected tissue, indicating that these effects are context dependent (Abtin et al., 2014). Collectively, these findings suggest that macrophages promote resolution of neutrophil-mediated inflammation at wounds by facilitating reverse migration.

To further determine whether macrophages promote neutrophil reverse migration, we identified the molecular pathways that mediate macrophage attraction to tissue damage. H_2O_2 is a reactive oxygen species (ROS) that has been shown to mediate neutrophil attraction to wounds (Niethammer et al., 2009). We recently identified the Src family kinase (SFK) Lyn as a sensor in neutrophils that detects H_2O_2 gradients generated by the dual oxidase (Duox) enzyme from epithelial wounds and mediates neutrophil attraction to wounds (Yoo et al., 2011). To determine whether ROS signaling mediates macrophage wound attraction, larvae were treated with the NADPH oxidase inhibitor, diphenyliodonium (DPI). Similarly to neutrophils, ROS inhibition strongly compromised the early recruitment of macrophages to wounds (1 h post–tail transection [hptt]). In contrast to neutrophils, ROS inhibition also impaired late (6 hptt) macrophage attraction to tissue damage (Fig. 3, A and B). In macrophages, ROS are mostly known to participate in phagocytosis and activation through autocrine processes (Brüne et al., 2013), but these findings suggest that the generation of hydrogen peroxide is also required for their motility and attraction to wounded tissues. This is in accordance with a recent study showing that Nox2 is required for macrophage chemotaxis in vitro (Chaubey et al., 2013).

To further test how ROS mediate macrophage-directed migration in vivo, we used *duox* MO to address the possible recruitment of macrophages by epithelium-generated H_2O_2 gradients and *cyba* MO to explore a possible role for self-generated sources of ROS. *duox* MO impaired macrophage recruitment at both 1 and 6 hptt (Fig. 3, C and D). Our results indicate that macrophage recruitment is dependent on wound-generated ROS, despite the presumed presence of other macrophage chemotactic factors released from inflammatory sites (Fredman and Serhan, 2011). The *cyba* MO targets the p22phox subunit of the Nox2 (NADPH oxidase complex 2) expressed in neutrophils and macrophages (Fig. S3, A and B), which is deficient in some forms of the human immunodeficiency chronic granulomatous disease (CGD; Stasia and Li, 2008). Depletion of p22phox also partially impaired macrophage recruitment, suggesting that macrophages may sustain their directed migration to tissue injury by producing their own source of ROS (Fig. 3, C and D). The findings indicate that macrophages exhibit a dual dependence on both extrinsic and intrinsic ROS for motility and wound attraction.

To investigate whether SFKs control macrophage-directed migration downstream of ROS in vivo, we characterized the role of macrophage SFKs in wound attraction. In contrast to neutrophils in which SFK are only important for early wound attraction, we found that SFK inhibition with PP2 impaired both early and late macrophage recruitment to wounds (Fig. 3, E and F). We previously showed that zebrafish macrophages express both Lyn and Yes-related kinase (Yrk) and that Lyn exerts a repressive

larvae fixed 1 and 6 hptt. (D) Quantification of macrophage recruitment to wounded fins of control, *duox* MO, or *cyba* MO larvae at the indicated times. (E) Representative images of 3-dpf Tg(*mpeg1:Dendra2*) larvae treated with 20 µM SFK inhibitor PP2 for 1 and 6 hptt. (F) Quantification of macrophage recruitment to wounded fins obtained in E. (G) Representative images of wild-type (control) 3-dpf Tg(*mpeg1:Dendra2*) larvae and *yrk* morphants #1 and #2 (*yrk* MO1 and *yrk* MO2) larvae fixed 1 and 6 hptt. (H) Quantification of macrophage recruitment to wounded fins in control, *yrk* MO1, and *yrk* MO2 larvae at 1 and 6 hptt. Ctrl, control. (*n*) = number of larvae. Horizontal lines indicate means. Error bars indicate SEM. *, $P < 0.05$; **, $P < 0.01$; ***, $P < 0.001$; ****, $P < 0.0001$, one-way ANOVA with Dunnett's post-test (B and H) and two-tailed unpaired *t* test (D and F). Dashed lines border the location of tail transection. Bars: (A and C) 60 µm; (E and G) 50 µm.

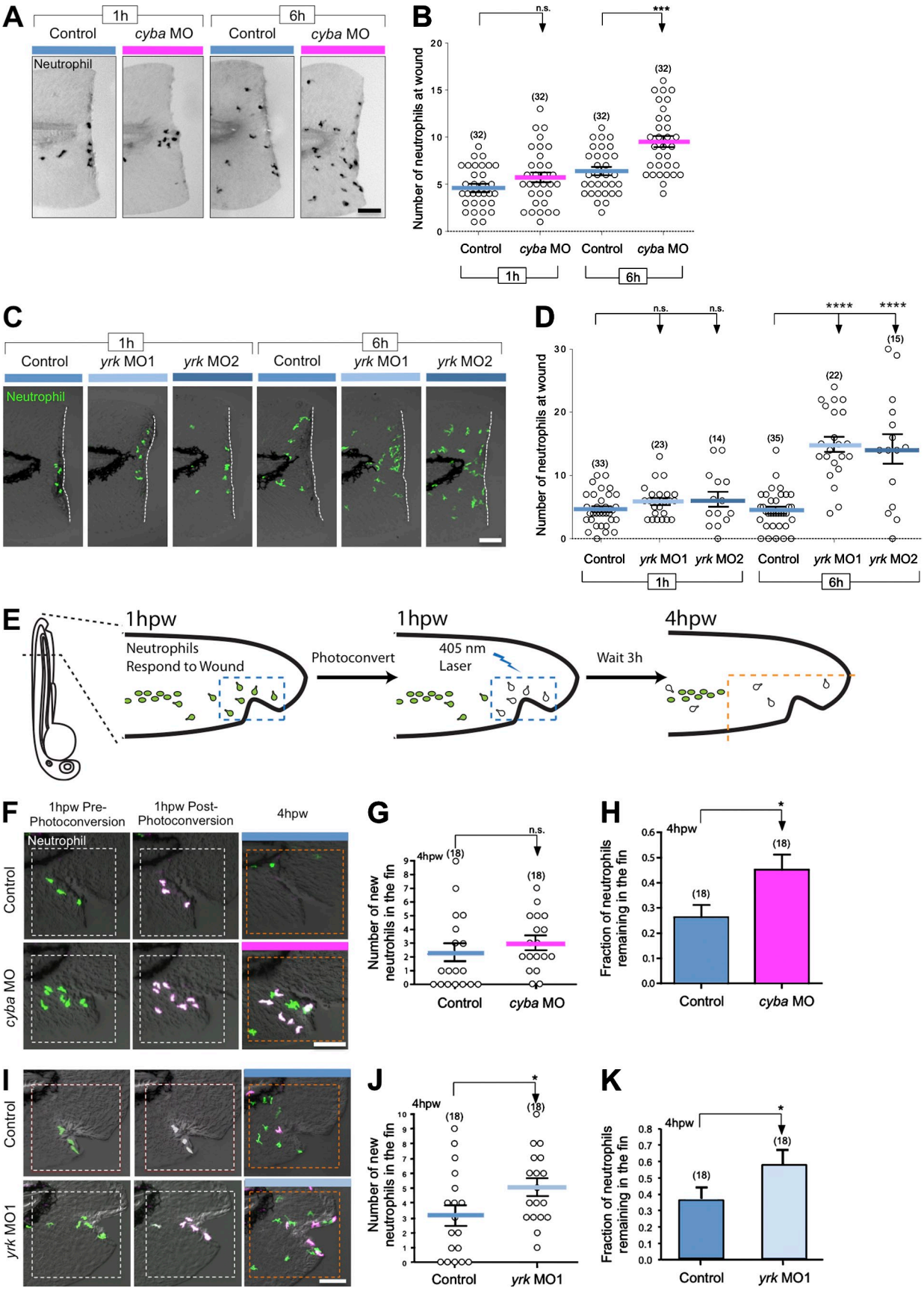

Figure 4. **p22 phox and Yrk regulate neutrophil reverse migration.** (A) Representative images of neutrophil recruitment to wounds in 3-dpf control and *cyba* morphant (*cyba* MO) larvae. 1 and 6 hptt, larvae were fixed, and Sudan black staining was used to visualize neutrophils. (B) Quantification of the number of neutrophils at wound in control and *cyba* morphant (*cyba* MO) larvae at 1 and 6 hptt. (C) Representative images of neutrophil recruitment to

effect on macrophage chemotaxis to wounds (Yoo et al., 2011). Yrk is expressed in macrophages but not neutrophils (Fig. S3 A) and was an attractive candidate to mediate macrophage recruitment. To test this idea, we depleted endogenous Yrk using two different MOs. Depletion of Yrk impaired early and late macrophage wound attraction, with a more significant effect noted 6 hptt (Fig. 3, G and H). Our findings identified a novel role for the SFK, Yrk, in macrophage wound attraction and help to clarify the complex interplay between SFK members in differentially tuning neutrophil and macrophage-directed migration in vivo (Meng and Lowell, 1998; Abram and Lowell, 2008; Baruzzi et al., 2008; Zhu et al., 2008; Byeon et al., 2012).

Macrophages and neutrophils both depend on ROS–SFK signaling for their early recruitment to wounds, but we found that ROS–SFK differentially regulate late neutrophil and macrophage wound recruitment (Yoo et al., 2011). It is an intriguing idea that the role of ROS–SFK signaling in neutrophil resolution may, in part, be indirect through macrophage regulation of neutrophil behavior. In accordance with this idea, patients with CGD who are deficient in NADPH oxidase or p22phox have increased neutrophil-mediated inflammation in tissues for unknown reasons (Stasia and Li, 2008). To investigate the role of leukocyte-produced ROS in neutrophil-mediated inflammation, we depleted p22phox using *cyba* MO and characterized the resolution of neutrophil-mediated inflammation. We found that p22phox was not important for initial neutrophil recruitment (Fig. 4, A and B). However, at 6 hptt, *cyba* morphants had significantly more neutrophils near the wound than controls using both needle wounding and tail transection (Fig. 4, A and B; and Fig. S3, D and F). Nonetheless, because p22phox is expressed in both macrophages and neutrophils (Fig. S3 A), it is not clear whether these effects are cell autonomous. Because we observed that *cyba* morphants had fewer macrophages and more neutrophils at the wound at late time points, we speculated that this was caused by having fewer macrophages present at the wound to repel neutrophils. To further determine whether macrophages regulate neutrophil infiltration, we examined neutrophil wound attraction in *yrk* morphants (Fig. S3 C), because Yrk is expressed specifically in macrophages but not neutrophils. We found that neutrophils were retained at wounds in *yrk* morphants at 6 hptt, with no effect on early wound attraction (Fig. 4, C and D). Collectively, these findings indicate that the presence of macrophages at wounds does not impact initial neutrophil wound recruitment but is required for proper resolution of neutrophil infiltration at sites of tissue damage.

To determine whether Yrk and p22phox specifically regulate neutrophil reverse migration to modulate resolution of neutrophil infiltration at wounds, we used Tg(*mpx:Dendra2*) zebrafish larvae, which express the photoconvertible protein, Dendra2, in neutrophils to specifically track the fate of wound-associated neutrophils in *cyba* or *yrk* morphants (Fig. 4 E; Yoo and Huttenlocher, 2011). Early neutrophil recruitment to the wound was not affected in *cyba* morphants (Fig. 4, A and B); however, we found that p22phox deficiency significantly impaired neutrophil reverse migration (Fig. 4, F and H). We found that *cyba* morphants had a slight, but nonsignificant, increase in the recruitment of new neutrophils to the wound area (Fig. 4 G), demonstrating that the persistent infiltration of neutrophils in the fins of *cyba* morphant larvae was a result of impaired reverse migration. In *yrk* morphants, we observed that both new neutrophil recruitment to the wound and impaired reverse migration of neutrophils contributed to impaired resolution of neutrophil inflammation (Fig. 4, I and K). Thus, we demonstrated that neutrophil reverse migration from wounds is reduced when macrophage wound response is impaired.

To determine a cell-autonomous role for *cyba*, we ectopically expressed MO-resistant *cyba* in either neutrophils or macrophages and analyzed neutrophil and macrophage wound recruitment in *cyba* morphants. Although ectopic expression of *cyba* in neutrophils impaired early neutrophil wound attraction, it did not rescue the reverse migration defect caused by *cyba* depletion (Fig. 5, A and B). However, ectopic expression of *cyba* in macrophages rescued both macrophage recruitment to wounds and the resolution of neutrophil-mediated inflammation (Fig. 5, C and D). These findings support a key role for macrophage redox signaling and macrophage recruitment in the resolution of neutrophil inflammation. Moreover, it is possible that in patients with CGD, persistent neutrophil infiltration may, in part, be caused by a defect in neutrophil resolution through a macrophage-dependent pathway.

Here, we demonstrate that macrophages are necessary for neutrophil reverse migration and resolution of neutrophil-mediated inflammation at wounds. We have identified a ROS-activated, SFK signaling pathway in macrophages that mediates macrophage recruitment to wounds and the subsequent egress of neutrophils from tissue damage. Parallel ROS-activated SFK signaling cascades are necessary for early neutrophil recruitment to wounds through Lyn (Yoo et al., 2011) and the regeneration of wounded tissues through Fyn (Yoo et al., 2012), implicating these ROS–SFK pathways in adjacent tissues as key regulators in multiple phases of the wound response (Fig. 5 E). We observed that macrophages frequently contact neutrophils before neutrophils move away from the wound, indicating a contact-mediated guidance that resembles the chase and run behavior reported for neural crest cells (Theveneau et al., 2013). Collectively, our findings suggest that redox-SFK signaling in

wounds in 3-dpf Tg(*mpx:Dendra2*) larvae treated with buffer control or *yrk* MO1 and *yrk* MO2 at 1 and 6 hptt. Dashed lines border the location of tail transection. (D) Quantification of the number of neutrophils at wounds in C. (E) Schematic of the reverse migration experiment (see Materials and methods). (F) Representative images acquired just before photoconversion, just after photoconversion, and at 4 hpw. 3-dpf Tg(*mpx:Dendra2*) larvae that were injected with buffer (control) or *cyba* MO were wounded. (G) Quantification of the number of new neutrophils entering the wounded fin area (bounded by dashed orange squares). (H) Quantification of the fraction of neutrophils remaining in the wounded area. (I) Same experimental setting as in F was used to compare neutrophil reverse migration between control and *yrk* MO1 larvae. (J) Graph representing the quantification of new neutrophils at the wound 4 hpw. (K) Histogram of the fraction of neutrophils remaining in the fin counted 4 hpw. (*n*) = number of larvae. Horizontal lines indicate means. Error bars indicate SEM. *, $P < 0.05$; ***, $P < 0.001$; ****, $P < 0.0001$, two-tailed unpaired *t* test (B, G, H, J, and K) and one-way ANOVA with Dunnett's post-test (D). Bars, 70 µm.

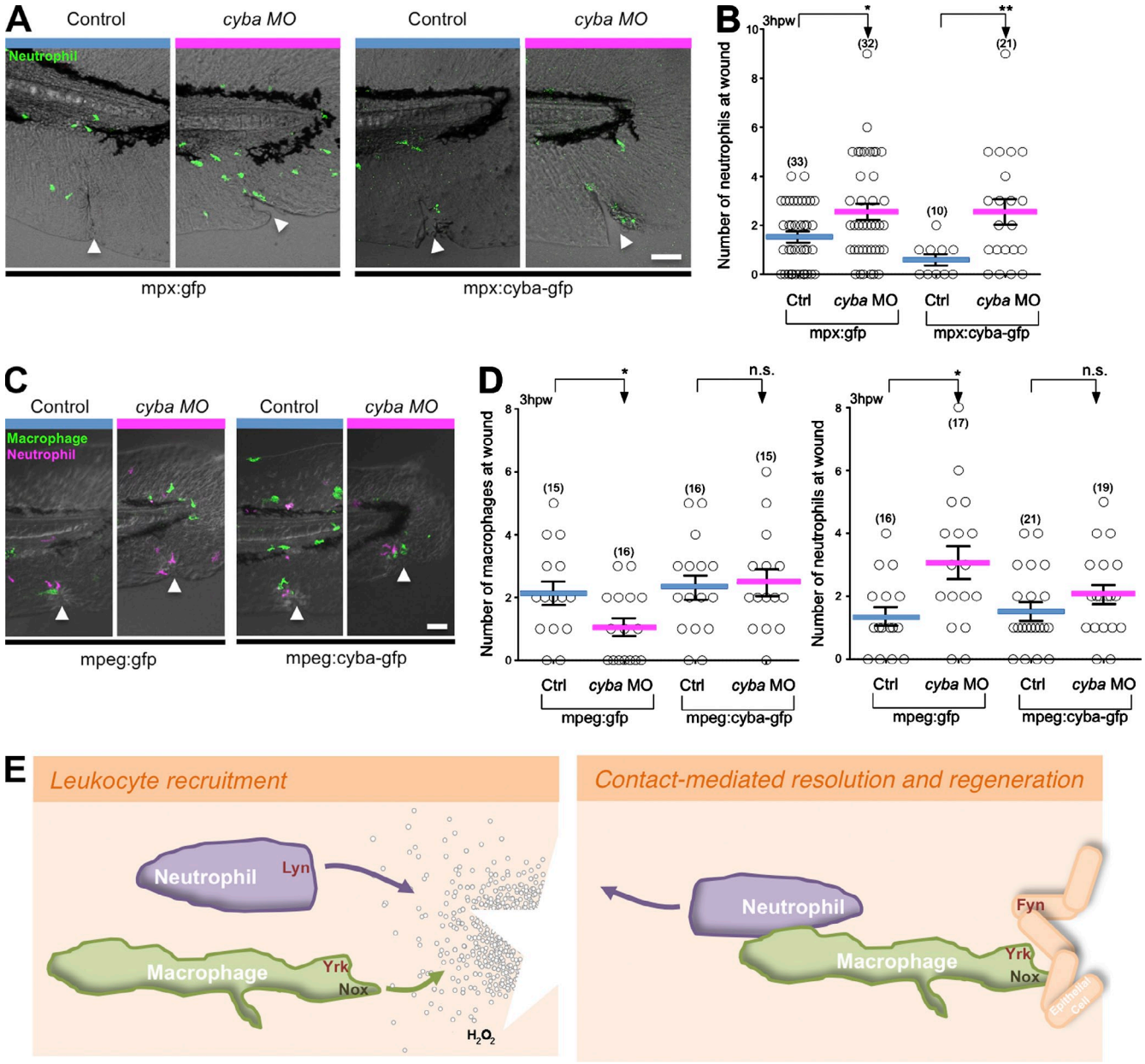

Figure 5. **p22 phox expression in macrophages regulates the neutrophil wound response.** (A) Representative images of neutrophil wound recruitment with or without *cyba* MO in 3-dpf Tg(*mpx:gfp*) or Tg(*mpx:cyba-gfp*) 3-dpf larvae fixed 3 hpw. (B) Quantification of the number of neutrophils at the wound obtained in A. (C) Representative images of neutrophil and macrophage wound recruitment 3 hpw with or without *cyba* MO in Tg(*mpx;mcherry*) larvae that transiently express *mpeg-gfp* or *mpeg:cyba-gfp* (D) Quantification of the number of macrophages (left) and neutrophils (right) present at 3 hpw in 3-dpf larvae depicted in C. Ctrl, control. (*n*) = number of larvae. Horizontal lines indicate means. Error bars indicate SEM. *, $P < 0.05$; **, $P < 0.01$, two-tailed unpaired *t* test. The triangles indicate wound location. Bars, 50 µm. (E) Schematic representation of redox/SFK signaling in adjacent tissues that control leukocyte recruitment to wounds (left), resolution of inflammation, and wound regeneration (right). After tissue injury, hydrogen peroxide (H_2O_2) is released and triggers the activation of the SFK Lyn in neutrophils. We report here that macrophages also require hydrogen peroxide production for their directed migration and identify the pivotal role of NADPH oxidase and the SFK Yrk in macrophage chemotaxis and indirectly on neutrophil reverse migration.

adjacent tissues is essential for coordinated leukocyte wound attraction and repulsion during the onset and resolution of inflammation induced by tissue damage.

Materials and methods

General zebrafish procedures and drug treatment

All adult and larval zebrafish were maintained according to protocols approved by the University of Wisconsin-Madison Institutional Animal Care and Use Committee. For wounding and live imaging assays, 3-d-postfertilization (dpf) larvae were anesthetized with E3-Tricaine (0.2 mg/ml Tricaine) medium. When indicated, 3-dpf larvae were pretreated with drug 1 h before experiments (indicated concentration of DPI and 20 µM PP2) in E3 with 0.1% DMSO. All drugs were purchased at EMD Millipore. Tail transections were performed with a razor blade. Ventral tailfin wounds were performed using a 33-gauge × 1/2-inch needle.

MO injection

3 nl of MO solution (Gene Tools) in Danieau buffer (58 mM NaCl, 0.7 mM KCl, 0.4 mM $MgSO_4$, 0.6 mM $Ca(NO_3)_2$, and 5 mM Hepes, pH 7.2) or Danieau buffer alone was injected into 1-cell-stage embryos. 100 µM *duox* splice MO (5′-AGTGAATTAGAGAAATGCACCTTTT-3′) was

injected with 300 µM *p53* MO (5′-GCGCCATTGCTTTGCAAGAATTG-3′), and 300 µM p53 MO alone was used as a control (Yoo et al., 2011). For p22phox knockdown, *cyba* (*cyba* is the p22phox gene) splice MO (5′-ATCATAGCATGTAAGGATACATCCC-3′) was used at 500 µM. Two *yrk* splice MOs were used, 500 µM *yrk* MO #1 (*yrk* MO1; 5′-GTCCTTCATCTGTAAACTCACGTGT-3′) and 500 µM *yrk* MO #2 (*yrk* MO2; 5′-CAATAACTGCACAAACGCACCTTTA-3′). 400 µM *irf8* MO (5′-AATGTTTCGCTTACTTGAAAATGG-3′) was used to deplete macrophages in larvae (Li et al., 2011). 500 µM *lyn* MO (5′-TCAGACAGCAAATAGTAATCACCTT-3′) was used as previously described (Yoo et al., 2011).

Transient expression of *mpeg:cyba-gfp*

3 nl of solution containing 20 ng/µl of DNA plasmid (*tol2-mpeg:cyba-gfp* or *tol2-mpeg:gfp* as a control) and 17 ng/µl of transposase mRNA with and without 500 µM of *cyba* MO in Danieau buffer was injected in Tg(*mpx;mcherry*) 1-cell-stage embryos. At 2 dpf, larvae were dechorionated and screened for double positive–expressing larvae.

RT-PCR

RNA was made from the individual larvae by dissociating them in 100 µl TRIZOL (Invitrogen) followed by centrifugation at 14,000 *g* for 10 min at 4°C. 20 µl CH_3Cl was added to the supernatant, vortexed in brief, and chilled on ice for 10 min. The sample was centrifuged for 20 min, and 35 µl of the upper, aqueous layer was collected. 35 µl isopropanol was added to the collected layer, mixed, and centrifuged for 10 min, and 70 µl of 70% ethanol in diethylpyrocarbonate H_2O was added followed by centrifugation for 10 min. The ethanol was decanted, and the RNA pellet was allowed to dry before resuspending it in 10 µl RNase-free water. RT-PCR was performed on purified RNA with a OneStep RT-PCR kit (QIAGEN) to assess the effectiveness of the *cyba* MO. A single reaction contained the following: 16.45 µl RNase-free H_2O, 5 µl of 5× reaction buffer, 1 µl deoxynucleotide triphosphate, 0.5 µl RNasin, 0.15 µl forward primer (100 µM stock), 0.15 µl reverse primer (100 µM stock), 1 µl enzyme mix, and 0.75 µl RNA. The following cycle was used: 53°C for 30 min, 95°C for 15 min, 33× (95°C for 30 s, 55°C for 60 s, and 72°C for 60 s), 72°C for 5 min, and hold at 4°C. The following primers were used (shown 5′ to 3′): *yrk* forward, CAGATCATGAAGAGGCTCCGTC; *yrk* reverse, CCTGCTCCAGCACCTCTCGG; *cyba* forward, ATGGCGAAGATTGAGTGGGCGAT; *cyba* reverse, GCTGCAGCATGGAGGTTATCTGCT; *mpeg1* forward, CTTTAATTCAGAGCCACGGAGGAGC; *mpeg1* reverse, GTAGACAACCCTAAGAAACCACAGG; *mpx* forward, GCTGCTGTTGTGCTCTTTCA; *mpx* rev, TTGAGTGAGCAGGTTTGTGG; *ef1a* forward, TACGCCTGGGTGTTGGACAAA; and *ef1a* reverse, TCTTCTTGATGTATCCGCTGA.

Sudan black staining and immunofluorescence

3-dpf larvae were anesthetized with E3-Tricaine and wounded as indicated in the General zebrafish procedures and drug treatment section. Tricaine was removed by washing the larvae with E3. The larvae were returned to a 28.5°C incubator for the indicated amount of time. Larvae were fixed with 4% paraformaldehyde in PBS overnight at 4°C and washed with PBS. They were incubated in Sudan black for 20–60 min and washed with 70% ethanol. Embryos were observed with a zoom stereomicroscope (SMZ1500; Nikon). For immunofluorescence, the indicated larvae were fixed with 1.5% formaldehyde in 0.1 M Pipes, 1.0 mM $MgSO_4$, and 2 mM EGTA overnight at 4°C and permeabilized in methanol as previously described (Yoo et al., 2011). Anti–MPEG-1 antibody from rabbit (#55917; AnaSpec) was used at 1:200 to label macrophages. DyLight 549–conjugated IgG antibody from goat (Jackson ImmunoResearch Laboratories, Inc.) was used as a secondary antibody.

Live imaging

Real-time imaging was performed on 3-dpf double transgenic larvae Tg(*mpx:DsRed*) × Tg(*mpeg1:Dendra2*) and Tg(*mpx:Dendra2*) larvae. The *mpeg1* and *mpx* promoters were used to specifically drive expression of fluorescent proteins in macrophages (Ellett et al., 2011) and neutrophils (Yoo et al., 2011), respectively. After needle wounding or tail transection, larvae were mounted in E3-Tricaine (0.2 mg/ml Tricaine) containing 1% low melting agarose. To track macrophage and neutrophil behavior, a z series stack of each larva was acquired at room temperature every 1–5 min during the indicated times using a laser-scanning confocal microscope (FluoView FV1000; Olympus) with an NA 0.75/20× objective using FV10-ASW as acquisition software (Olympus). Manual tracking was performed with the MTrackJ plug-in for ImageJ software (National Institutes of Health). When indicated, directionality corresponds to the distance between the origin and final point of the neutrophil track compared with the total distance traveled by the same neutrophil. For Fig. 2 (B–G), the behavior of neutrophils at the wound was analyzed in 89 videos; 54 were useable for quantification. 16 videos exhibit neutrophils first at wound (condition a), and 16 were quantified (n = 20 different neutrophil tracks). 23 videos exhibit macrophages first at wound (condition b), and 13 were quantified (n = 60 different neutrophil tracks). In the remaining 15 videos, neutrophils and macrophages reach the wound simultaneously. For Fig. 2 (E–G), the percentage of neutrophils that resolved = (number of neutrophils that touched the wound and reverse migrated during a 2-h acquisition)/(total number of neutrophils that touched the wound) × 100. For Fig. 2 (H–K), the results were obtained from the analysis of five different larvae for the control and three different larvae for the *irf8* MO. For Fig. 2 (E–K), results are representative of three independent experiments.

Reverse migration assay

Tg(*mpx:Dendra2*) zebrafish embryos were treated as indicated in the figures and as described in general zebrafish procedures and drug treatment section. Dendra2 is a photoconvertible fluorescence protein whose emission can be permanently changed from green to red by excitation with 405-nm light (Gurskaya et al., 2006). Batches of control and morphant larvae were wounded as described in the General zebrafish procedures and drug treatment section. At 1 or 2 hpw, larvae were mounted in E3-Tricaine (0.2 mg/ml Tricaine) containing 1% low melting agarose. An imaging sequence was performed on each larva that involved taking one initial z stack of the tailfin, photoconverting the neutrophils around the tailfin, and taking a second z stack immediately after photoconversion. Photoconversion was performed at 1 or 2 h after wounding in a region of interest around the wounded or transected area that were approximately the same size for each larva. The following stimulation settings were used for photoconversion: 40% 405-nm laser transmissivity, 10 µs/pixel dwell time, and 45 s total stimulation time. After all larvae were photoconverted, the larvae were imaged to determine the position of the neutrophils at the indicated time points. A region that was determined dorsally by the tip of the notochord and cranially by the distal end of the caudal artery (Fig. 4 E, diagram) was used to determine the number of neutrophils remaining in the wounded area at 4 hpw. The number of new neutrophils was determined by taking the difference of the number of nonphotoconverted neutrophils in this region at 1 and 4 hpw. For the tail transection model, the region used to determine the number of photoconverted neutrophils remaining in the wounded area corresponded with the same area used for photoconversion.

Statistical tests

All statistical tests were performed using Prism (GraphPad Software). Comparisons between two groups were performed with two-tail unpaired *t* test. For comparisons among three or more groups, one-way analysis of variance (ANOVA) with Dunnett's post-test was used. Error bars indicate SEM. Each result is representative of at least three independent experiments.

Online supplemental material

Fig. S1 shows the kinetics of neutrophil–macrophage interactions at wounds. Fig. S2 shows that macrophage depletion increases neutrophil inflammation. Fig. S3 shows that *cyba* is necessary for resolution of neutrophil-mediated inflammation. Video 1 shows the kinetics of neutrophil–macrophage interactions at wounds. Video 2 shows that neutrophils are repelled by macrophages. Video 3 shows the neutrophil behavior at wounds is influenced by macrophages. Video 4 shows a macrophage chasing a neutrophil at the wound edge. Video 5 shows a neutrophil chased by a macrophage. Video 6 shows that neutrophils avoid macrophages to arrive at the wound. Video 7 shows the trapping and phagocytosis of a neutrophil by a macrophage. Video 8 shows a neutrophil trapped by a macrophage at the wound. Video 9 shows that *irf8* morphant larvae exhibit impaired neutrophil reverse migration. Video 10 shows the disorganized neutrophil migration in *irf8* morphant. Online supplemental material is available at http://www.jcb.org/cgi/content/full/jcb.201408090/DC1.

This work was supported by the American Heart Association postdoctoral fellowship 13POST16190005 (S. Tauzin), National Institutes of Health grant GM074827 (A. Huttenlocher), National Institutes of Health F30 fellowship HL114143, National Institutes of Health grant HL007899, and National Institutes of Health grant GM008692 (T.W. Starnes).

The authors declare no competing financial interests.

Submitted: 22 August 2014
Accepted: 4 November 2014

References

Abercrombie, M. 1967. Contact inhibition: the phenomenon and its biological implications. *Natl. Cancer Inst. Monogr.* 26:249–277.

Abram, C.L., and C.A. Lowell. 2008. The diverse functions of Src family kinases in macrophages. *Front. Biosci.* 13:4426–4450. http://dx.doi.org/10.2741/3015

Abtin, A., R. Jain, A.J. Mitchell, B. Roediger, A.J. Brzoska, S. Tikoo, Q. Cheng, L.G. Ng, L.L. Cavanagh, U.H. von Andrian, et al. 2014. Perivascular macrophages mediate neutrophil recruitment during bacterial skin infection. *Nat. Immunol.* 15:45–53. http://dx.doi.org/10.1038/ni.2769

Baruzzi, A., E. Caveggion, and G. Berton. 2008. Regulation of phagocyte migration and recruitment by Src-family kinases. *Cell. Mol. Life Sci.* 65:2175–2190. http://dx.doi.org/10.1007/s00018-008-8005-6

Bratton, D.L., and P.M. Henson. 2011. Neutrophil clearance: when the party is over, clean-up begins. *Trends Immunol.* 32:350–357. http://dx.doi.org/10.1016/j.it.2011.04.009

Brüne, B., N. Dehne, N. Grossmann, M. Jung, D. Namgaladze, T. Schmid, A. von Knethen, and A. Weigert. 2013. Redox control of inflammation in macrophages. *Antioxid. Redox Signal.* 19:595–637. http://dx.doi.org/10.1089/ars.2012.4785

Byeon, S.E., Y.S. Yi, J. Oh, B.C. Yoo, S. Hong, and J.Y. Cho. 2012. The role of Src kinase in macrophage-mediated inflammatory responses. *Mediators Inflamm.* 2012:1–18. http://dx.doi.org/10.1155/2012/512926

Chaubey, S., G.E. Jones, A.M. Shah, A.C. Cave, and C.M. Wells. 2013. Nox2 is required for macrophage chemotaxis towards CSF-1. *PLoS ONE.* 8:e54869. http://dx.doi.org/10.1371/journal.pone.0054869

Ellett, F., L. Pase, J.W. Hayman, A. Andrianopoulos, and G.J. Lieschke. 2011. mpeg1 promoter transgenes direct macrophage-lineage expression in zebrafish. *Blood*. 117:e49–e56. http://dx.doi.org/10.1182/blood-2010-10-314120

Fredman, G., and C.N. Serhan. 2011. Specialized proresolving mediator targets for RvE1 and RvD1 in peripheral blood and mechanisms of resolution. *Biochem. J.* 437:185–197. http://dx.doi.org/10.1042/BJ20110327

Gurskaya, N.G., V.V. Verkhusha, A.S. Shcheglov, D.B. Staroverov, T.V. Chepurnykh, A.F. Fradkov, S. Lukyanov, and K.A. Lukyanov. 2006. Engineering of a monomeric green-to-red photoactivatable fluorescent protein induced by blue light. *Nat. Biotechnol.* 24:461–465. http://dx.doi.org/10.1038/nbt1191

Holmes, G.R., G. Dixon, S.R. Anderson, C.C. Reyes-Aldasoro, P.M. Elks, S.A. Billings, M.K. Whyte, V. Kadirkamanathan, and S.A. Renshaw. 2012. Drift-diffusion analysis of neutrophil migration during inflammation resolution in a zebrafish model. *Adv. Hematol.* 2012:1–8. http://dx.doi.org/10.1155/2012/792163

Li, L., H. Jin, J. Xu, Y. Shi, and Z. Wen. 2011. Irf8 regulates macrophage versus neutrophil fate during zebrafish primitive myelopoiesis. *Blood*. 117:1359–1369. http://dx.doi.org/10.1182/blood-2010-06-290700

Li, L., B. Yan, Y.Q. Shi, W.Q. Zhang, and Z.L. Wen. 2012. Live imaging reveals differing roles of macrophages and neutrophils during zebrafish tail fin regeneration. *J. Biol. Chem.* 287:25353–25360. http://dx.doi.org/10.1074/jbc.M112.349126

Mathias, J.R., B.J. Perrin, T.X. Liu, J. Kanki, A.T. Look, and A. Huttenlocher. 2006. Resolution of inflammation by retrograde chemotaxis of neutrophils in transgenic zebrafish. *J. Leukoc. Biol.* 80:1281–1288. http://dx.doi.org/10.1189/jlb.0506346

Meng, F., and C.A. Lowell. 1998. A β1 integrin signaling pathway involving Src-family kinases, Cbl and PI-3 kinase is required for macrophage spreading and migration. *EMBO J.* 17:4391–4403. http://dx.doi.org/10.1093/emboj/17.15.4391

Nathan, C. 2006. Neutrophils and immunity: challenges and opportunities. *Nat. Rev. Immunol.* 6:173–182. http://dx.doi.org/10.1038/nri1785

Nathan, C., and A. Ding. 2010. Nonresolving inflammation. *Cell*. 140:871–882. http://dx.doi.org/10.1016/j.cell.2010.02.029

Niethammer, P., C. Grabher, A.T. Look, and T.J. Mitchison. 2009. A tissue-scale gradient of hydrogen peroxide mediates rapid wound detection in zebrafish. *Nature*. 459:996–999. http://dx.doi.org/10.1038/nature08119

Ortega-Gómez, A., M. Perretti, and O. Soehnlein. 2013. Resolution of inflammation: an integrated view. *EMBO Mol. Med.* 5:661–674. http://dx.doi.org/10.1002/emmm.201202382

Robertson, A.L., G.R. Holmes, A.N. Bojarczuk, J. Burgon, C.A. Loynes, M. Chimen, A.K. Sawtell, B. Hamza, J. Willson, S.R. Walmsley, et al. 2014. A zebrafish compound screen reveals modulation of neutrophil reverse migration as an anti-inflammatory mechanism. *Sci. Transl. Med.* 6:225ra29. http://dx.doi.org/10.1126/scitranslmed.3007672

Silva, M.T. 2010. When two is better than one: macrophages and neutrophils work in concert in innate immunity as complementary and cooperative partners of a myeloid phagocyte system. *J. Leukoc. Biol.* 87:93–106. http://dx.doi.org/10.1189/jlb.0809549

Sindrilaru, A., and K. Scharffetter-Kochanek. 2013. Disclosure of the culprits: macrophages-versatile regulators of wound healing. *Adv Wound Care (New Rochelle)*. 2:357–368. http://dx.doi.org/10.1089/wound.2012.0407

Starnes, T.W., and A. Huttenlocher. 2012. Neutrophil reverse migration becomes transparent with zebrafish. *Adv. Hematol.* 2012:1–11. http://dx.doi.org/10.1155/2012/398640

Stasia, M.J., and X.J. Li. 2008. Genetics and immunopathology of chronic granulomatous disease. *Semin. Immunopathol.* 30:209–235. http://dx.doi.org/10.1007/s00281-008-0121-8

Stramer, B., S. Moreira, T. Millard, I. Evans, C.Y. Huang, O. Sabet, M. Milner, G. Dunn, P. Martin, and W. Wood. 2010. Clasp-mediated microtubule bundling regulates persistent motility and contact repulsion in *Drosophila* macrophages in vivo. *J. Cell Biol.* 189:681–689. http://dx.doi.org/10.1083/jcb.200912134

Theveneau, E., B. Steventon, E. Scarpa, S. Garcia, X. Trepat, A. Streit, and R. Mayor. 2013. Chase-and-run between adjacent cell populations promotes directional collective migration. *Nat. Cell Biol.* 15:763–772. http://dx.doi.org/10.1038/ncb2772

Woodfin, A., M.B. Voisin, M. Beyrau, B. Colom, D. Caille, F.M. Diapouli, G.B. Nash, T. Chavakis, S.M. Albelda, G.E. Rainger, et al. 2011. The junctional adhesion molecule JAM-C regulates polarized transendothelial migration of neutrophils in vivo. *Nat. Immunol.* 12:761–769. http://dx.doi.org/10.1038/ni.2062

Yoo, S.K., and A. Huttenlocher. 2011. Spatiotemporal photolabeling of neutrophil trafficking during inflammation in live zebrafish. *J. Leukoc. Biol.* 89:661–667. http://dx.doi.org/10.1189/jlb.1010567

Yoo, S.K., T.W. Starnes, Q. Deng, and A. Huttenlocher. 2011. Lyn is a redox sensor that mediates leukocyte wound attraction in vivo. *Nature*. 480:109–112. http://dx.doi.org/10.1038/nature10632

Yoo, S.K., C.M. Freisinger, D.C. LeBert, and A. Huttenlocher. 2012. Early redox, Src family kinase, and calcium signaling integrate wound responses and tissue regeneration in zebrafish. *J. Cell Biol.* 199:225–234. http://dx.doi.org/10.1083/jcb.201203154

Zhu, J.W., T. Brdicka, T.R. Katsumoto, J. Lin, and A. Weiss. 2008. Structurally distinct phosphatases CD45 and CD148 both regulate B cell and macrophage immunoreceptor signaling. *Immunity*. 28:183–196. http://dx.doi.org/10.1016/j.immuni.2007.11.024